BIOCHEMISTRY
including biophysical chemistry & molecular biology

ARTICLE

pubs.acs.org/biochemistry

Identification and Physicochemical Characterization of BldR2 from *Sulfolobus solfataricus*, a Novel Archaeal Member of the MarR Transcription Factor Family

Gabriella Fiorentino,[*,†] Immacolata Del Giudice,[†] Simonetta Bartolucci,[†] Lorenzo Durante,[‡] Luigi Martino,[§] and Pompea Del Vecchio[*,‡]

[†]Department of Structural and Functional Biology, University of Naples Federico II, Edificio 7, via Cinthia, 80126 Naples, Italy

[‡]Department of Chemistry "Paolo Corradini", University of Naples Federico II, via Cinthia, 80126 Naples, Italy

[§]Randall Division of Cell and Molecular Biophysics, King's College London, New Hunt's House, Guy's Campus, London SE1 1UL, U.K.

Supporting Information

ABSTRACT: The multiple antibiotic resistance regulators (MarR) constitute a family of ligand-responsive transcriptional regulators abundantly distributed throughout the bacterial and archaeal domains. Here we describe the identification and characterization of BldR2, as a new member of this family, in the archaeon *Sulfolobus solfataricus* and report physiological, biochemical, and biophysical investigation of its stability and DNA binding ability. Transcriptional analysis revealed the upregulation of *BldR2* expression by aromatic compounds in the late-logarithmic growth phase and allowed the identification of *cis*-acting sequences. Our results suggest that BldR2 possesses in solution a dimeric structure and a high stability against both temperature and chemical denaturing agents; the protein binds site specifically to its own promoter, *Sso1082*, with a micromolar binding affinity at two palindromic sites overlapping TATA-BRE and the transcription start site. Benzaldehyde and salicylate, ligands of MarR members, are antagonists of binding of DNA by BldR2. Moreover, two single-point mutants of BldR2, R19A and A65S, properly designed for obtaining information about the dimerization and the DNA binding sites of the protein, have been produced and characterized. The results point out an involvement of BldR2 in the regulation of the stress response to aromatic compounds and point to arginine 19 as a key amino acid involved in protein dimerization, while the introduction of serine 65 increases the DNA affinity of the protein, making it comparable with those of other members of the MarR family.

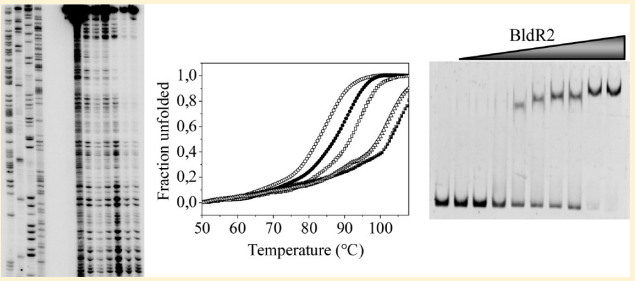

Archaea, the third domain of life, are microorganisms adapted to grow in extreme environments with regard to temperature, pH, ionic strength, and high concentrations of detergents and organic solvents.[1] They are an evolutionary mosaic, being more similar to eukaryotes with respect to the macromolecular machinery and more similar to bacteria with respect to metabolic systems and genome organization.[2−4] For example, with regard to the transcription machinery, in most cases, homologues of bacterial regulators function in the context of the archaeal basal transcriptional apparatus, which resembles that of Eukarya. Archaea possess a TATA box promoter sequence, a TATA box-binding protein (TBP), a homologue of the transcription factor TFIIB (TFB), and an RNA polymerase (RNAP) containing between 8 and 13 subunits.[5,6]

Archaea have been of interest to many protein chemists over the years, as models for understanding the molecular basis of adaptation to extreme conditions. In the case of adaptations to extremes of pH, salinity, and pressure, it has been proven that membrane components and protective small molecules may play important roles.[7] However, with regard to temperature adaptations, the cellular components themselves, namely the proteins, have to achieve thermostability.[8,9] Like all other living cells, archaea are also able to defend against subtle changes to environmental conditions; they own in their genomes finely regulated biochemical pathways for detoxification as well as different regulative sequences responsive to stress agents.[10−13] The multiple antibiotic resistance regulators (MarR) constitute a family of ligand-responsive transcriptional regulators that are distributed throughout the bacterial and archaeal domains and include proteins critical for the control of virulence factor production, the response to oxidative stress, and the regulation of the catabolism of environmental aromatic compounds. They are also involved in the regulation of mechanisms of resistance to multiple antibiotics, organic solvents, household disinfectants, and pathogenic factors. MarR homologues are dimeric proteins that have a low level of sequence identity and a triangular shape; they

Received: February 4, 2011
Revised: June 28, 2011
Published: June 30, 2011

bind to their cognate palindromic or pseudopalindromic DNA as homodimers, resulting in either transcriptional repression or activation.[14] The DNA binding domain of MarR proteins is a conserved winged helix−turn−helix motif[15] with the two wings located at the corners of the triangle. Another common feature of MarR members is their ability to interact with specific ligands and, upon binding, to modulate DNA recognition.[16] Crystal structures of several MarR regulators have been obtained, either as apoproteins, in complex with the cognate DNA, or with various effectors, greatly contributing to the elucidation of the mechanistic basis of DNA and/or ligand binding. However, the identification of key residues involved in binding as well as those contributing to protein stability and/or dimerization has been reported only in a few cases.[17−19]

In the archaeal domain, the crystal structures of four transcription factors, ST1710 (or StEmrR) from *Sulfolobus tokodaii*,[20,21] MTH313 from *Methanobacterium thermoautotrophicum*,[22] PH1061 from *Pyrococcus horikoshii* OT3,[23] and BldR from *Sulfolobus solfataricus*,[24] have been determined. The overall structure of all of these proteins is typical of the MarR family, particularly for elements taking part in the DNA-binding domain, while the most important differences are found in the dimerization domain. The structures of MTH313 and ST1710 complexed with salicylate as the ligand revealed conservation of the ligand binding pocket.[17,22] Furthermore, it has been proposed that the ability to act as activators or repressors could not be related to a particular DNA binding mechanism, but rather to the position of the binding site on the target DNA.[24] Comparison of the thermophilic StEmrR with mesophilic MarR showed an increase in the number of salt bridges on the protein surface predicted to be important in increasing the thermostability.[21]

Some of us identified *BldR* as part of an operon-like structure conserved in most archaea. Functional characterization demonstrated that BldR is a transcriptional activator involved in the detoxification of aromatic compounds.[25,26] The *S. solfataricus* genome contains an additional ORF, *Sso1082*, that encodes another putative MarR protein of 154 amino acids that is 35% identical in sequence to BldR of the same organism.

In this work, we have performed a physiological and biochemical analysis of BldR2 with the aim of enhancing our knowledge of the role of MarR proteins in the archaeal domain. Our results showed that the gene is transcriptionally regulated. Furthermore, BldR2 is a homodimer that binds specifically to its own promoter in a region that overlaps with the sequences recognized by the basal transcription machinery. In the presence of benzaldehyde and salicylate, ligands of MarR members, BldR2 dissociates from its promoter. In this study, we also report interesting results in terms of conformational stability and DNA binding properties of BldR2 through biophysical and biochemical measurements. Moreover, to provide further insights into thermal stability and DNA binding molecular mechanisms of BldR2, we used guided mutagenesis based on the structure of the close relatives BldR[24] and ST1710[21] and identified two residues, Arg19, possibly involved in dimer stabilization, and Ala65, located in the DNA binding domain. BldR has in the same position a serine residue directly involved in DNA binding.[24] These two residues, Arg19 and Ala65, were substituted in two different mutants with Ala and Ser, respectively, and a complete characterization was conducted in parallel with wild-type BldR2.

MATERIALS AND METHODS

S. solfataricus Cultivation and Preparation of Genomic DNA and Total RNA. *S. solfataricus* P2 was grown aerobically at 82 °C in 100 mL of medium described by Brock supplemented with 0.1% (w/v) yeast extract and 0.1% (w/v) casamino acids[27] and buffered at pH 3.5. In some cases, benzaldehyde, sodium salicylate, and benzyl alcohol were added to final concentrations of 1, 0.35, and 4 mM, respectively, after dilution of an exponentially growing culture up to an A_{600} of 0.08 optical density (OD) unit. Cells were grown to ∼0.3 and ∼0.7 OD_{600} unit, corresponding to midlogarithmic and late-logarithmic phases, respectively, and harvested by centrifugation at 4000*g* for 10 min. Genomic DNA and total RNAs were prepared following reported procedures.[28]

In Vivo Response to Aromatic Compounds. RNAs (10 μg) extracted from cells grown under different conditions were electrophoretically separated in a 1.5% agarose gel containing 10% formaldehyde and transferred to nylon filters (GE Healthcare). Hybridization was conducted as described by Cannio et al.,[28] using the *Sso1082* and *Sso1352* genes[25] and rRNA 16S as probes. The experiments were performed in duplicate. Signals were visualized by autoradiography and quantified with a densitometric analysis using a Personal Fx phosphorimager and Quantity One (Bio-Rad).

Primer Extension Analysis of the Transcription Start Site. To determine the first transcribed nucleotide, total RNA extracted from cells grown in the presence or absence of benzaldehyde and harvested at 0.3 OD_{600} unit was subjected to primer extension analysis as described by Limauro et al.,[29] using primer *Sso1082+100Rv* (5′-GGC CTA TTT GCT CAA GAG CC-3′), annealing from position 100 bp in the *Sso1082* gene. The same primer was used to produce a sequence ladder by using the f-Mol DNA cycle sequencing system (Promega), according to the manufacturer's instructions, to locate the products on a 6% urea−polyacrylamide gel.

Heterologous Expression of _Sso1082_ and Purification of the Recombinant Protein. The gene encoding *Sso1082* from *S. solfataricus* P2 was amplified by polymerase chain reaction (PCR) from genomic DNA, using *Pfx* DNA polymerase. Two different upstream primers both containing the *Nde*I restriction site (underlined) (*Sso1082up*, 5′-GGA TTT TGT GAG TTCATATGA TG-3′; *Sso1082Fw*, 5′-GTT AGA TAT CTA CAT ATG ATA TTA GC-3′) were designed on the basis of two different putative translation start sites. In particular, *Sso1082Ssoup* anneals to the ATG annotated on the genome[30] while *Sso1082Fw* anneals to another putative start codon located 45 nucleotides downstream and deduced from both a transcriptomic analysis[31] and our primer extension. The common downstream primer *Sso1082 Rev* (5′-GCT TTA AGA CTC GAG TAG TTA GG-3′) introduces a stop codon and the *Xho*I restriction site (underlined in the sequence). Amplified fragments were purified, digested with appropriate restriction enzymes, and cloned in the pET30a *Nde*I- and *Xho*I-modified vector, generating pET30*Sso1082*long and pET30*Sso1082*, respectively. The sequences of the two cloned fragments were shown to be identical to those available on the *S. solfataricus* P2 genome (http://www-archbac.u-psud.fr/projects/sulfolobus/).

Escherichia coli BL21-CodonPlus (DE3) cells (Stratagene) transformed with pET30*Sso1082*long and pET30*Sso1082* were used for recombinant protein expression.

Cells transformed with pET30*Sso1082* were grown in 1 L of Luria-Bertani medium containing kanamycin (100 μg/mL) and chloramphenicol (33 μg/mL). When the culture reached an A_{600} of 0.5 OD unit, protein expression was induced by the addition of 0.5 mM IPTG and the bacterial culture grown for an additional 6 h. Cells were harvested by centrifugation, and pellets were lysed by sonication in 30 mL of lysis buffer [50 mM Tris-HCl (pH 8.0) and 1 mM phenylmethanesulfonyl fluoride] in an ultrasonic liquid processor (Heat system Ultrasonic Inc.). The lysate was centrifuged at 30000*g* for 60 min (SW41 rotor, Beckman). The supernatant was heated to 80 °C for 10 min, and denatured proteins were precipitated by centrifugation at 20000*g* for 20 min at 4 °C.

The supernatant was loaded onto a heparin column (5 mL, HiTrap heparin, GE Healthcare) equilibrated in 50 mM Tris-HCl (pH 8.0) (buffer A) connected to an AKTA Explorer system (GE Healthcare). After a washing step with buffer A, elution was conducted with 40 mL of a KCl gradient (0 to 0.8 M). Fractions containing the BldR2 protein were pooled, concentrated, dialyzed, and loaded onto a Superdex 75 column (26 cm × 60 cm, GE Healthcare) equilibrated in 50 mM Tris-HCl (pH 8.0) and 0.2 M KCl (buffer B) at a flow rate of 2 mL/min. Fractions were collected and analyzed by SDS−PAGE to detect the BldR2 protein. These fractions were pooled, concentrated by ultrafiltration using a YM10 membrane (Millipore), dialyzed against buffer A, and stored at 4 °C.

Construction, Expression, and Purification of R19A and A65S Mutants. Single-point mutations in the *BldR2* gene were produced with the Quick Change Site-Directed Mutagenesis Kit (Stratagene) that utilizes *PfuUltra* high-fidelity DNA polymerase and primers complementary to the coding and noncoding template sequences.

To generate the R19A and A65S mutants, the forward primers (*FwSso1082*R19A, 5′-TTGGGATCTAATAACTGGACTGACAGCAAAGATAAATAAGGATACAGATAAG-3′; *FwSso1082* A65S, 5′-GCTGAAAAATATATGCTGACAAAGTCGGGATTAACTAGCATCATT-3′) with their complementary reverse primers were used (underlined letters indicate the base pair mismatch) and reactions performed according to the manufacturer's instructions. The mutagenesis products were transformed into XL-1 Blue Cells. Single colonies were selected on LB plates containing kanamicin, and isolated plasmidic DNAs were sequenced at Eurofins MWG Operon.

Plasmids pET30R19A and pET30A65S containing the desired mutations were used to transform BL21 Codon plus (DE3) competent cells. The best growth conditions for gene expression were determined both for cells transformed with pET30R19A and for cells transformed with pET30A65S: growth to an OD_{600} of ∼0.5 and ∼0.8 in LB medium supplemented with kanamycin (50 μg/mL) and chloramphenicol (33 μg/mL) at 37 °C, respectively, followed by induction for 6 h with 0.5 mM IPTG.

The purification of the mutant proteins was conducted in a manner similar to that already described for the wild-type BldR2 protein.

Computational Methods. To establish similarities among the sequences of proteins of interest and the sequences of the SwissProt Data Bank, computational analysis was performed at http://www-arch-bac.u-psud.fr/projects/sulfolobus/ or http://cmr.jcvi.org/cgi-bin/CMR/GenomePage.cgi?org=ntss02, providing access to the genome of *S. solfataricus* P2.

The multiple-sequence alignment was obtained using T-COFFEE.[32] The three-dimensional (3D) model of BldR2 has been built with EsyPred3D using the BldR 3D structure as a template.[33]

Analytical Methods for Protein Characterization and Sample Preparation. Protein concentrations were determined by the method of Bradford, using BSA as the standard.[34] Protein homogeneity was estimated by SDS−PAGE [12.5% (w/v) gels]. To determine the native molecular mass of the proteins, the purified proteins at different concentrations (0.25, 0.5, 1.5, and 3.0 mg/mL) were applied in a volume of 100 μL to an analytical Superdex PC75 column (3.2 cm × 30 cm) connected to an AKTA Explorer system (GE Healthcare) alternatively equilibrated with buffer B, with 20 mM sodium phosphate (pH 7.5) and 0.2 M KCl, or with the same buffer used for EMSA (see below), at a flow rate of 0.04 mL/min. The column was calibrated in the different buffers using a set of gel filtration markers (low range, GE Healthcare), including bovine serum albumin (67.0 kDa), ovalbumin (43.0 kDa), chymotrypsinogen A (25.0 kDa), and RNase A (13.7 kDa). The molecular mass of the protein and mutants was also determined using electrospray mass spectra recorded on a Bio-Q triple quadrupole instrument (Micromass, Thermo Finnigan, San Jose, CA).

Protein solutions for spectroscopic analyses were prepared in a 20 mM sodium phosphate buffer (pH 7.5), and the concentration was determined by UV spectra using a theoretical, sequence-based extinction coefficient of 22920 M^{-1} cm^{-1} calculated at 280 nm for the dimeric protein.[35] A commercial 8 M GuHCl solution from Sigma was used as a denaturant solvent. Protein solutions for CD and fluorescence measurements were exhaustively dialyzed by using Spectra Por membranes (molecular weights of 15000−17000) against buffer solution at 4 °C. The water used for buffer and sample solutions was doubly distilled. The pH was measured at 25 °C with a Radiometer model PHM93 pH meter.

Samples for GuHCl-induced denaturation experiments were prepared with increasing amounts of denaturing agent. Each sample was mixed by vortexing and incubated at 4 °C for 1 day. Longer incubation times produced identical spectroscopic signals.

Cloning of *Sso1082* Promoter Regions. Two different regions upstream of the ORF *Sso1082* were amplified by PCR amplification on *S. solfataricus* P2 genomic DNA: the first of 230 bp was obtained using the primer pair *Sso1082fw-130* (5′-ATT AGG ATA TAG ATC TCG TTT ACG A-3′) and *Sso1082 +100Rv*. The *Sso1082prFw* primer anneals starting at position −130 with respect to the transcription initiation site as determined by primer extension analysis.

A second smaller region of 164 bp was amplified with the pair *Sso1082fw-130* (see above) and *Sso1082+34Rv* (5′-CCCAAACTTCTGAGTACTTTGTAG-3′) annealing from position +34 in the *Sso1082* gene.

The fragments were cloned in the pGEM T-easy vector (Promega) and TopoTA (Invitrogen) to give *Sso1082L* (large) and *Sso1082S* (small), respectively. The insertion and correct sequence of the PCR products were verified by DNA sequencing.

DNA Binding. Binding of BldR2, R19A, and A65S to the putative regulatory region *Sso1082L* was measured by an electrophoretic mobility shift assay (EMSA) using a biotin-labeled PCR fragment amplified from the pGEM T-easy vector using the *Sso1082Fw-130* and the *Sso1082+100Rv* primers (see above). The amplified DNA fragment was labeled at the 3′-OH end with the Biotin 3′ End DNA labeling kit (Thermo Scientific), according to the manufacturer's protocol.

EMSA reaction mixtures were set up in a final volume of 15 μL and contained 5 nM DNA, 1 μg of poly(dI-dC), and varying amounts of proteins in binding buffer [25 mM Tris-HCl (pH 8), 50 mM KCl, 10 mM $MgCl_2$, 1 mM dithiothreitol, and 5% glycerol]. The mixtures were incubated at 60 °C for 20 min and run onto a nondenaturing 5% polyacrylamide gel (Bio-Rad) in 1× TBE at 80 V. The probes were transferred onto a positively charged nylon membrane (Hybond-XL, GE Healthcare, Uppsala, Sweden) with a blotting apparatus (Bio-Rad, Hercules, CA) and then detected with the Chemiluminescent Nucleic Acid Detection Module Kit (Thermo Scientific) according to the kit protocol.

To determine the dissociation constants of BldR2, R19A, and A65S with respect to the *Sso1082* promoter, the *Sso1082S* regulatory region (150 nM) was incubated with increasing amounts of the purified proteins and the complexes were separated as described above; after electrophoresis, gels were directly stained with SYBR green (nucleic acid gel stain, Invitrogen). At least two independent experiments were performed in duplicate. In particular, protein concentrations (in dimer units) ranged from 1.0 to 90 μM for BldR2 and R19A and from 0.05 to 1.5 μM for A65S.

Densitometric data were obtained with Quantity One (Bio-Rad) and manipulated to calculate the fractional complex formation (that is the ratio between the density of the retarded band and the total density, reported in percent). These values were analyzed by fitting the binding isotherm to the Hill equation in GraphPad Prism 5.0.

To analyze the effect of benzaldehyde and salicylate on the properties of BldR2, R19A, and A65S binding to the *Sso1082S* promoter, EMSAs were performed via preincubation of the proteins, at concentrations similar to their apparent K_d values, with 3, 5, 10, 20, 30, 50, and 100 mM sodium salicylate or benzaldehyde. Gels were processed and visualized as described above.

DNase I Footprinting. A probe containing the promoter region of the *Sso1082* gene was produced by PCR using a combination of the *Sso1082 ftR* primer (5′-CGAATTCGCCCTT-**GGGTTTGAAG**-3′) designed on the basis of the *Sso1082* promoter (bold) and pTopo sequences, respectively, starting at +34 bp from the transcription initiation site, and *Sso1082*−*184* (5′-CCATATTTATAATCTCTACA-3′) as a second primer; the latter was labeled at the 5′ end with T4 polynucleotide kinase and [γ-^{32}P]ATP. The labeled PCR product of 231 bp (∼40 nM) was incubated with 5−10 μg of pure BldR2, R19A, and A65S at 60 °C in binding buffer (see above) and digested with 1 unit of DNase I (Ambion) for 1 min at 37 °C. Subsequent steps were performed as described by Fiorentino et al.[25] Labeled primer was as also used to generate a dideoxynucleotide sequence ladder with the Promega f-Mol DNA sequencing system using *Sso1082S-Topo* (see above) as the template and following the manufacturer's instructions.

Circular Dichroism and Fluorescence Measurements. CD spectra were recorded with a Jasco J-715 spectropolarimeter equipped with a Peltier-type temperature control system (model PTC-348WI). The molar ellipticity per mean residue, $[\theta]$ in degrees square centimeters per decimole, was calculated from the equation $[\theta] = ([\theta]_{obs}mrw)/(10lC)$, where $[\theta]_{obs}$ is the ellipticity measured in degrees, mrw is the mean residue molecular weight (117.6) for protein BldR2, C is the protein concentration in grams per milliliter, and l is the optical path length of the cell in centimeters. Cells with path lengths of 0.1 and 1 cm were used in the far-UV and near-UV regions, respectively. CD spectra were recorded with a time constant of 4 s, a 2 nm bandwidth, and a scan rate of 20 nm/min; the signal was averaged over at least three scans and baseline corrected by subtraction of a buffer spectrum. Spectra were analyzed for secondary structure amount according to the CDSSTR method[36] using Dichroweb.[37] The GuHCl-induced denaturation curves, at a fixed constant temperature of 25 °C, were obtained by recording the CD signal at 230 nm for the samples containing increasing amounts of GuHCl. Finally, the thermal unfolding curves were recorded in the temperature mode, by following the change in the CD signal at 222 nm with a scan rate of 1.0 °C/min. Fluorescence measurements were performed with a JASCO FP-750 apparatus equipped with a circulating water bath to keep the cell holders at a constant temperature of 25 °C. The denaturant-induced unfolding curves were obtained by recording changes in both fluorescence intensity and fluorescence maximal wavelength as a function of GuHCl concentration. The excitation wavelength was set to 290 nm, and the experiments were performed by using a 1 cm sealed cell and a 5 nm emission slit width and corrected for the background signal. The change in fluorescence intensity at 336 nm was recorded to monitor the unfolding transition. The protein concentration was kept constant at 2.4 μM.

Analysis of the Denaturant-Induced Unfolding Transitions. For comparison of the denaturant-induced unfolding curves obtained in both the CD and fluorescence experiments, the curves were normalized reporting the fraction of unfolded protein (f_U) as a function of the concentration of the denaturing agent.

Thermodynamic parameters for the denaturant-induced unfolding were determined by analyzing the transition curves on the basis of a simple two-state model for dimeric proteins. In the equilibrium, only folded dimeric protein N_2 and unfolded monomers U exist. At any point in the denaturation reaction, the equilibrium costant K_U was calculated according to the model

$$K_U = [U]^2/[N_2] = 2P_t(f_U{}^2)/(1 - f_U) \quad (1)$$

in which P_t is the total molar concentration of protein monomers. The midpoint of the unfolding transition, C_m, was calculated using the equation

$$C_m = [RT \ln(P_t) + \Delta G_U(H_2O)]/m$$

The unfolding Gibbs energies were calculated using the relation

$$\Delta G_U = -RT \ln K_U \quad (2)$$

where R is the gas constant and T the absolute temperature. The linear dependence of the Gibbs energy of unfolding on the denaturant concentration is given by

$$\Delta G_U = \Delta G_U(H_2O) + m[D] \quad (3)$$

where $\Delta G_U(H_2O)$ is the extrapolated Gibbs energy of unfolding in the absence of denaturant[38] and m is the cooperativity parameter.[39] Values of $\Delta G_U(H_2O)$ were obtained directly by fitting the unfolding curves to eqs 1−3.

RESULTS

Transcriptional Analysis of *Sso1082*. Northern blot experiments were performed to verify the transcription of the *Sso1082* gene in two growth phases and to analyze transcription in cells grown in the presence of aromatic compounds, benzaldehyde, benzyl alcohol, and salicylate; these compounds were already demonstrated to inhibit cell growth at 1.5, 4, and 0.5 mM,

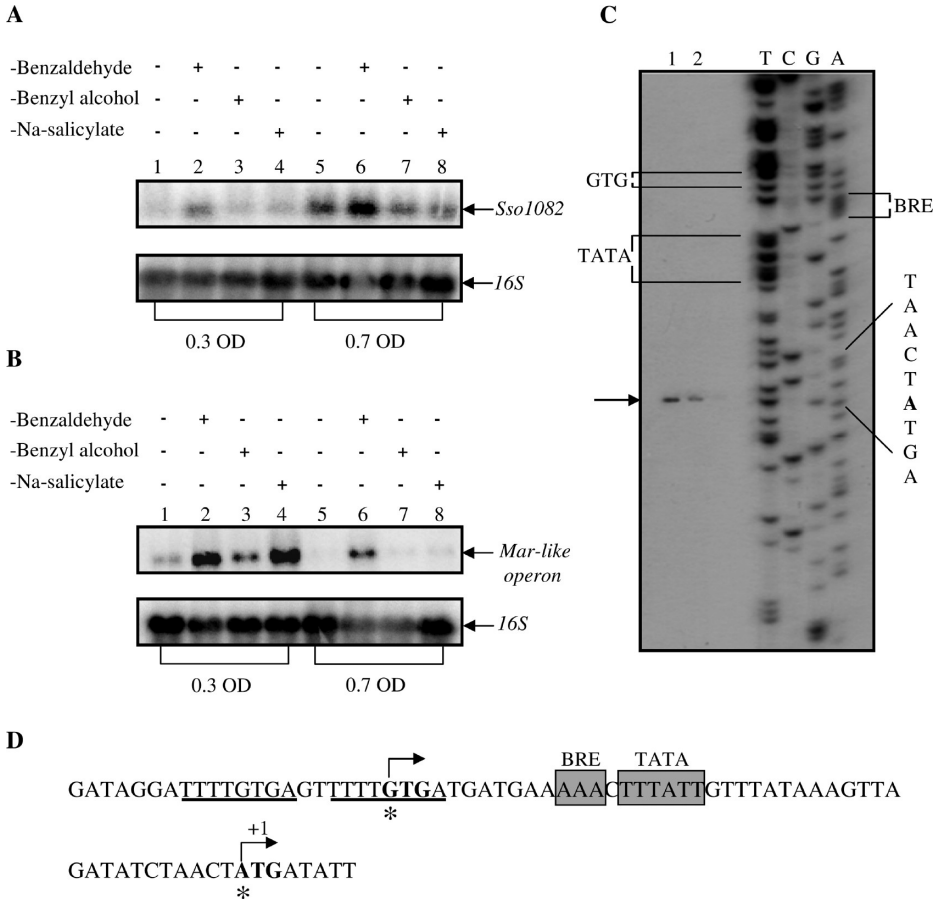

Figure 1. Transcriptional analysis of the *Sso1082* gene. Northern blot analysis of *Sso1082* (A) and *Mar-like* operon (B) mRNAs. Total RNA was prepared from *S. solfataricus* cells grown in the presence of different aromatic compounds and harvested in exponential (lanes 1−4) and stationary (lanes 5−8) growth phases: lanes 1 and 5, untreated control cells; lanes 2 and 6, cells grown in the presence of 1 mM benzaldehyde; lanes 3 and 7, cells grown in the presence of 4 mM benzyl alcohol; lanes 4 and 8, cells grown in the presence of 0.35 mM salicylate. The filters were probed with the *Sso1082* (A) and *Sso1352* (B) genes. Amounts of the mRNAs were normalized to 16S rRNA. The experiments were performed in duplicate. (C) Primer extension analysis of the *Sso1082* promoter region. Total RNA was prepared from cells grown in the presence (lane 1) or absence (lane 2) of benzaldehyde and harvested in the exponential growth phase. Primer-extended products were separated by electrophoresis under denaturing conditions alongside sequencing reactions with the same primer. (D) Promoter sequence analysis. The mapped transcription/translation start site (+1) is highlighted in bold; TBP and TFB binding sites are boxed. The initiation codon as annotated on the *S. solfataricus* genome is in bold and TSS as determined by Wurtzel are indicated by an asterisk.

respectively, and to affect *MarR-like operon* transcription.[25] The *BldR2* expression pattern was compared to that of the *MarR-like operon* and the 16S rRNA. *BldR2* mRNA revealed a single hybridization band under all the conditions tested with a molecular transcript of ~400 bp, which is slightly lower than that deduced from the gene sequence (462 bp) but is in accordance with a monocistronic transcript (Figure 1A). A densitometric analysis (Figure S1 of the Supporting Information) revealed that the level of *Sso1082* mRNA was ~3-fold higher in cells grown in the late exponential growth phase in comparison with that of cells grown in the early exponential growth phase (Figure 1A and Figure S1 of the Supporting Information, lanes 1 and 5).

Furthermore, the level of the transcript increased ~2-fold in cells grown in the presence of 1 mM benzaldehyde in comparison with nontreated cells in both growth phases (Figure 1A and Figure S1 of the Supporting Information, lanes 1, 2, 5, and 6). A weak induction could be observed when challenging cells with 4 mM benzyl alcohol (Figure 1A and Figure S1 of the Supporting Information, lanes 1−3 and 5−7) or 0.35 mM salicylate (Figure 1A and Figure S1 of the Supporting Information, lanes 1−4 and 5−8). The amounts of total cellular RNA were comparable in all the experiments, which could be judged by hybridization of the same filters with the 16S rRNA gene. Taken together, these results are evidence that the level of *Sso1082* expression increases in a later growth stage with respect to that of the *MarR-like operon* and responds to stress by aromatic drugs (Figure 1B).

To determine the transcription start site of *Sso1082*, a primer extension analysis was undertaken on RNAs prepared from cells grown in the presence or absence of benzaldehyde. Unexpectedly, the results presented in Figure 1C reveal that the transcription start site corresponds to an adenosine located 45 bp downstream of the GTG start codon annotated on the *S. solfataricus* P2 genome.[30] Interestingly, a recent report on the *S. solfataricus* transcriptome has revealed that *Sso1082* transcription starts at two major positions: one is located in position −1 relative to the beginning of the ORF annotated on the genome and a second that coincides with the one we mapped and overlaps a putative ATG start codon; the two transcripts would produce proteins in the same frame differing for 15 amino acids at the N-terminus.[31] It was also found that the extent of transcription from the downstream start site was >10-fold higher.[31]

dx.doi.org/10.1021/bi200187j |*Biochemistry* 2011, 50, 6607–6621

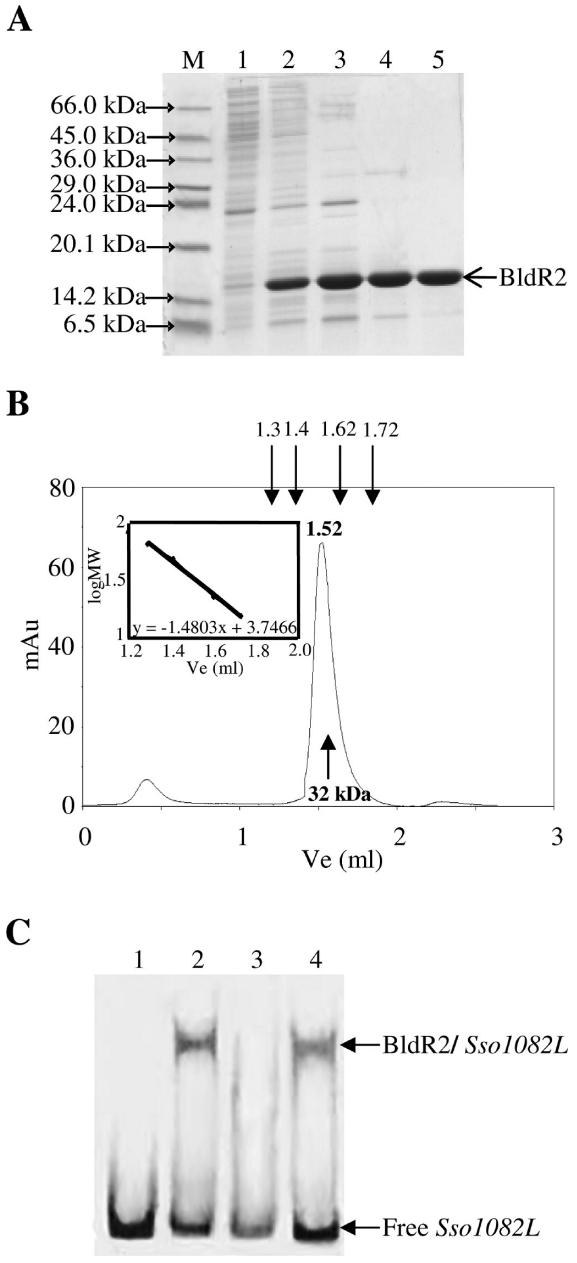

Figure 2. Analysis of recombinant BldR2. (A) SDS−PAGE of the purification steps of recombinant BldR2: lane M, molecular mass markers; lane 1, crude extract; lane 2, heat-treated cell extract; lane 3, fraction from heparin chromatography; lane 4, fraction from exclusion molecular chromatography; lane 5, purified BldR2. (B) Elution profile of purified BldR2 from gel filtration on a Superdex PC75 column. Recombinant BldR2 is eluted at 1.52 mL corresponding to a molecular mass of 32 kDa. Arrows indicate the elution volumes of the protein standards in the relative calibration of the column. (C) EMSA. *Sso1082L* (5 nM) and BldR2 incubated in the presence of specific and nonspecific competitors: lane 1, labeled DNA fragment; lane 2, DNA probe and BldR2 (15 μM); lane 3, *Sso1082L*, BldR2, and 1250 nM nonlabeled *Sso1082L* fragment; lane 4, *Sso1082L*, BldR2, and 1250 nM nonlabeled *gfp* fragment.

However, under all of our growth conditions, we detected only the shorter transcript. It is tempting to speculate that under our experimental conditions transcription and translation start sites could coincide, giving rise to a single transcript, and in vivo, a mature protein could be also translated starting from a Met residue located downstream from that found in the genome annotation.

The hypothesis is strengthened by the fact that the transcriptome study proved that leaderless translation is the preferred strategy in *S. solfataricus*.[31] On the basis of the position of the downstream transcription start site, it was possible to identify TATA box and BRE sequences perfectly matching with the consensus, located downstream of the predicted GTG initiation codon (Figure 1D). The results depicted in Figure 1C confirm the relative increase in the level of mRNA upon benzaldehyde induction.

Heterologous Expression and Characterization of BldR2. Both putative *Sso1082* genes predicted from genome annotation[26] and from the transcriptional analysis[31] were cloned in pET30 and expressed in *E. coli*; interestingly, BldR2 was expressed in *E. coli* as a soluble protein only when the corresponding gene was cloned from the downstream start codon. All of our attempts to produce a soluble protein from the gene sequence as annotated in the *S. solfataricus* genome failed;[30] the protein purified from inclusion bodies was also found to be very sensitive to protease degradation at its N-terminus. Edman sequencing revealed, in fact, the absence of the first 13 amino acids (data not shown).

Hence, in the following description, we refer to BldR2 as the smaller protein translated from the downstream transcription and translation start site, and the reported characterization has been performed on this protein. BldR2 was purified to homogeneity (Figure 2A), taking advantage of its intrinsic properties, including its thermostability, its putative DNA binding capability, and its small size. Active fractions were selected on the basis of their ability to shift their own promoter region, *Sso1082L*, spanning positions −130 to 100 relative to its transcription and translation initiation codon in an EMSA (see also below). From 1 L of *E. coli* culture, it was possible to obtain up to 20 mg of pure BldR2. The molecular mass of the recombinant BldR2 as determined by MS analysis was 16348 Da, in agreement with the corresponding theoretical value, and the same applies to the mutants. The quaternary structure was assessed via analytical gel filtration and revealed a homodimeric structure both at different protein concentrations and in different buffers (Figure 2B and Figure S2 of the Supporting Information), a result consistent with other MarR homologues.[15]

Specific Binding of BldR2 to Its Promoter Region. Because the majority of MarR transcription factors are autoregulators that bind site-specifically to their promoters, we assessed whether BldR2 had such a capacity. An EMSA confirmed that BldR2 was able to bind to this region (Figure 2C, lane 2) and revealed the specificity of the interaction; in fact, a *gfp* gene fragment[26] at a 250-fold molar excess could not compete for BldR2 binding (Figure 2C, lane 4), whereas an unlabeled specific competitor abolished gel retardation when added at the same ratio (Figure 2C, lane 3). Hence, this result shows that BldR2 specifically recognizes its own promoter.

Structural and Functional Characterization of BldR2 and Its Mutants. A multiple-sequence alignment of BldR2 with archaeal MarR members whose structure is known and comparison with bacterial representatives identified four identical residues, namely, Leu29, Leu74, Thr97, and Gly100 (Figure 3A). Leu29, Thr97, and Gly100 are located in helices α1 and α5 in the dimerization domain, while Leu74 is in helix α4 in the DNA binding domain.[13,24] Residues Glu75, Arg89, and Glu95,

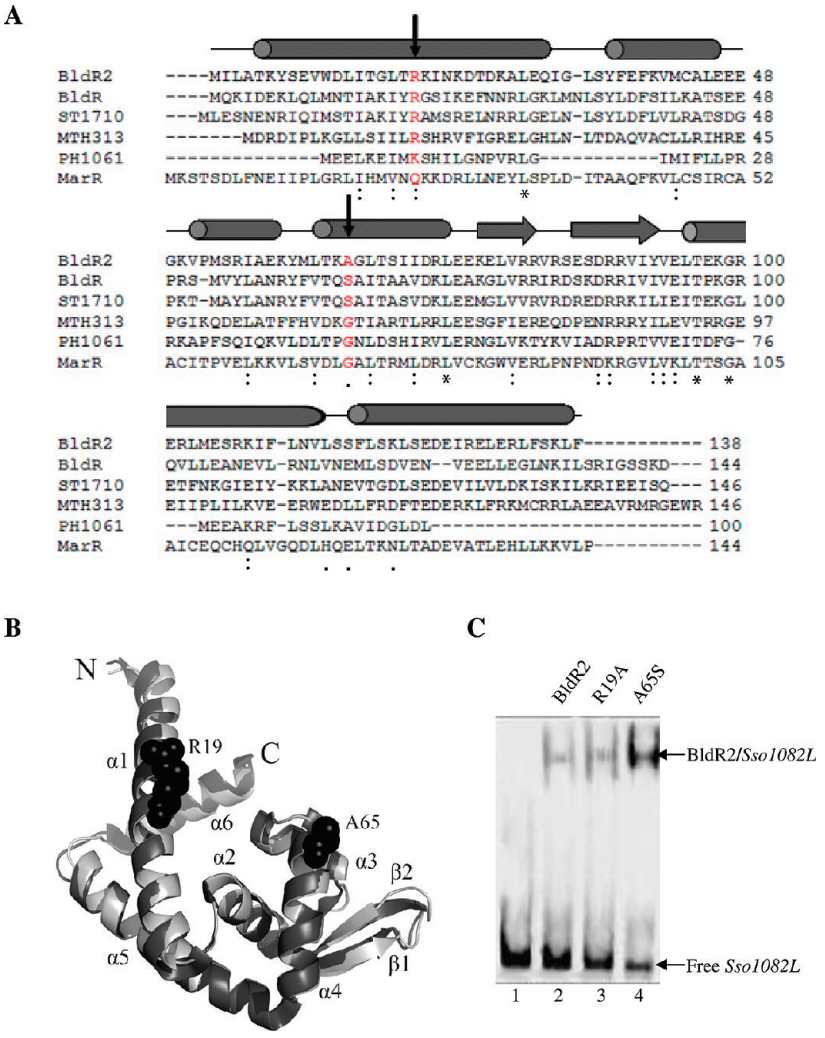

Figure 3. (A) Multiple-sequence alignment of BldR2 (*Sso1082*) with characterized MarR members. Proteins are BldR (*Sso1352*) from *S. solfataricus*, ST1710 from *S. tokodaii*, MTH313 from *M. thermoautotrophicum*, PH1061 from *P. horikoshii*, and MarR from *E. coli*. The secondary structure elements of BldR2 are depicted above the sequences. The mutations introduced by site-directed mutagenesis are highlighted by arrows. (B) Superposition of the 3D structure of the monomer of BldR (dark gray, Protein Data Bank entry 3F3X) and the 3D model of BldR2 (light gray). The mutated residues are shown as gray spheres. (C) Binding of purified BldR2, R19A, and A65S to the *Sso1082L* promoter region: lane 1, *Sso1082L*; lane 2, *Sso1082L* and 15 μM BldR2; lane 3, *Sso1082L* and 15 μM R19A; lane 4, *Sso1082L* and 15 μM A65S.

occurring in strand β3 (the wing motif), are identical only in the archaeal domain. Hence, on the basis of sequence analysis, BldR2 is expected to share a function similar to that of the other family members.

Sequence analysis of BldR2 from *S. solfataricus*, in comparison with its closest homologue, BldR, from the same organism, provided further information for the design of mutants that could help shed light on the structural properties and functions of BldR2. On the basis of the homology sequence shared between BldR and BldR2, we used the known 3D structure of BldR as a reference model for BldR2 (Figure 3B).[24] By also looking at the sequence alignment of Figure 3A, we found that some of the key residues important for dimer stabilization and DNA interaction in BldR are present in BldR2. Among these, the arginine in position 19 has been found to be conserved in known archaeal representatives. In most members with known structure, the Arg residue is in helix α1 of the dimerization domain and is located at the dimer interface where it contributes to dimer stability.[15,24] Furthermore, BldR2 has an alanine in position 65 instead of a serine that is conserved in BldR and ST1710 and is involved in DNA binding.[17,24] To investigate the contribution of these two amino acids to the DNA binding properties as well as the stability of BldR2, two mutants were generated. In the first, the arginine at position 19 was substituted with an alanine; in the second, the alanine at position 65 was substituted with a serine. For each of the single mutants, we performed a characterization in parallel with the wild-type protein. The mutants were overexpressed in *E. coli* and purified using the same procedure described for the wild-type enzyme. Native gel filtration revealed their ability to form dimers, suggesting that the mutations introduced did not alter the monomer−monomer interactions (Figure S2 of the Supporting Information). To verify whether the mutations affected the DNA binding capability of BldR2, we employed EMSAs using the *Sso1082L* promoter as the target DNA. Figure 3C shows that both mutants retained their activity, again indicating that the mutations were not disruptive. Interestingly, an increased intensity of the shifted band could be observed when the promoter region was incubated with identical amounts

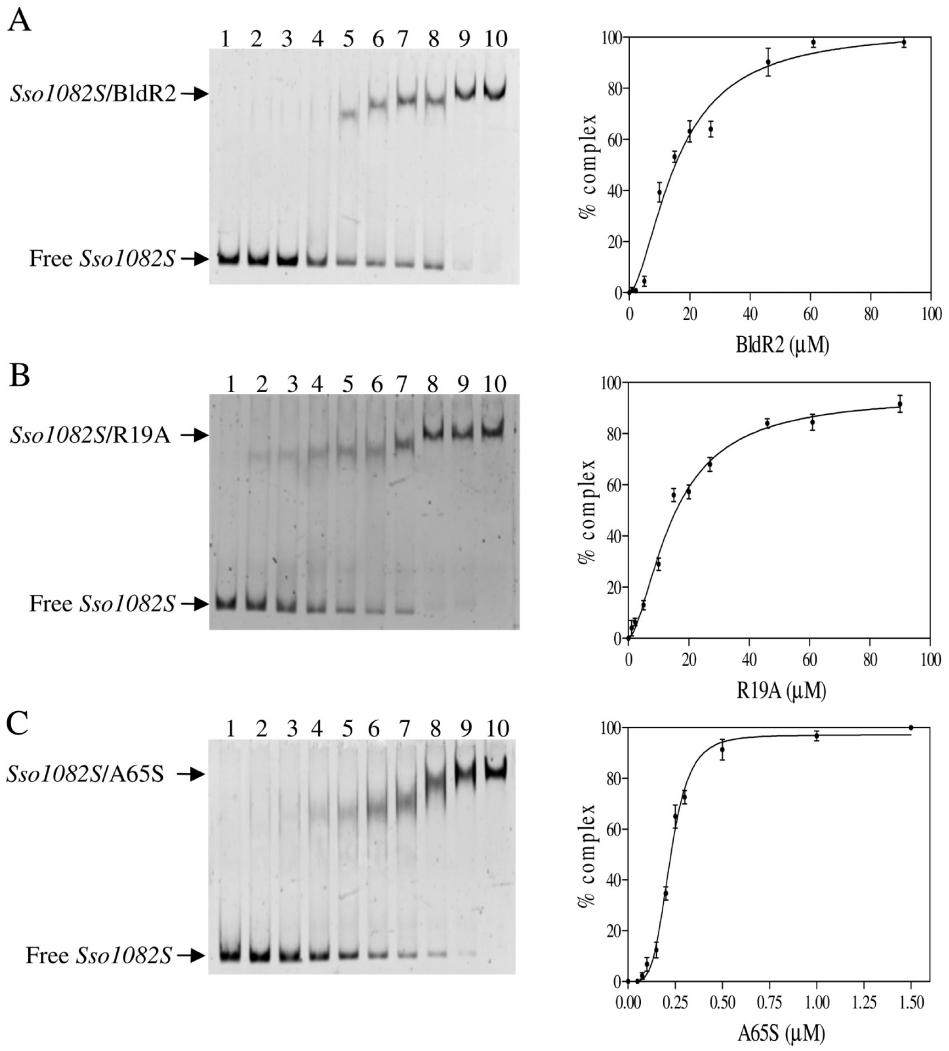

Figure 4. Binding of BldR2, A65S, and R19A to the *Sso1082* promoter assessed by an EMSA. (A) *Sso1082S* (150 nM) titrated with increasing concentrations of BldR2: lane 1, labeled DNA fragment; lanes 2−10, DNA probe incubated with BldR2 at concentrations ranging from 1.5 to 91 μM. (B) *Sso1082S* (150 nM) titrated with increasing concentrations of R19A: lane 1, labeled DNA fragment; lanes 2−9, *Sso1082S* incubated with R19A at concentrations ranging from 1.5 to 91 μM. (C) *Sso1082S* (150 nM) titrated with increasing concentrations of A65S: lane 1, labeled DNA fragment; lanes 2−9, *Sso1082pr* incubated with A65S at concentrations ranging from 0.05 to 1.5 μM. Densitometric data from EMSA obtained as described in Materials and Methods are plotted vs the concentration of each protein (right of each panel). Error bars represent the standard deviation for each point derived from four experiments.

of the A65S mutant (Figure 3C, lane 4) with respect to the wild-type protein (lane 2) and R19A (lane 3).

DNA Interaction Studies. To gain insight into the biological role of BldR2, we analyzed in more detail its DNA binding compared to that of its mutants, testing by an EMSA their binding affinity for an *Sso1082* promoter region, spanning positions −184 to +34 relative to the transcription and translation initiation codon (*Sso1082S*).

Titrations with increasing amounts of the BldR2 dimer indicated that the protein binds its own control region in a concentration-dependent manner; furthermore, at saturating concentrations, the protein determined a shift with decreased mobility, suggesting either that more binding sites with different affinities could exist in the DNA sequence analyzed or that multiple dimers could associate to the cognate DNA. The profile obtained by fitting densitometric data to a binding curve with a Hill slope gave an overall apparent equilibrium dissociation constant (K_d) of 15.8 μM (Figure 4A and Table 1) and provided a Hill coefficient of 1.7. A comparable binding pattern (Figure 4B) with a similar global affinity (K_d = 16.3 μM) and slope (1.6) was observed for the R19A mutant, while mutation of A65 to serine significantly changed the DNA binding properties; in fact, formation of a complex with A65S was seen using much lower protein concentrations (Figure 4C), and fitted binding data indicated an ∼70-fold increased affinity for the target promoter (K_d = 0.22 μM) and a slope of 4.3. These results clearly suggested that A65S binds with high affinity and via a different mechanism with respect to those of BldR2 and R19A.

Table 1. Dissociation Constants Calculated by EMSA for BldR2, R19A, and A65S with the *Sso1082* Promoter

	BldR2	R19A	A65S
Sso1082S	15.8 ± 5.2 μM	16.3 ± 4.5 μM	0.22 ± 0.02 μM

dx.doi.org/10.1021/bi200187j |*Biochemistry* 2011, 50, 6607–6621

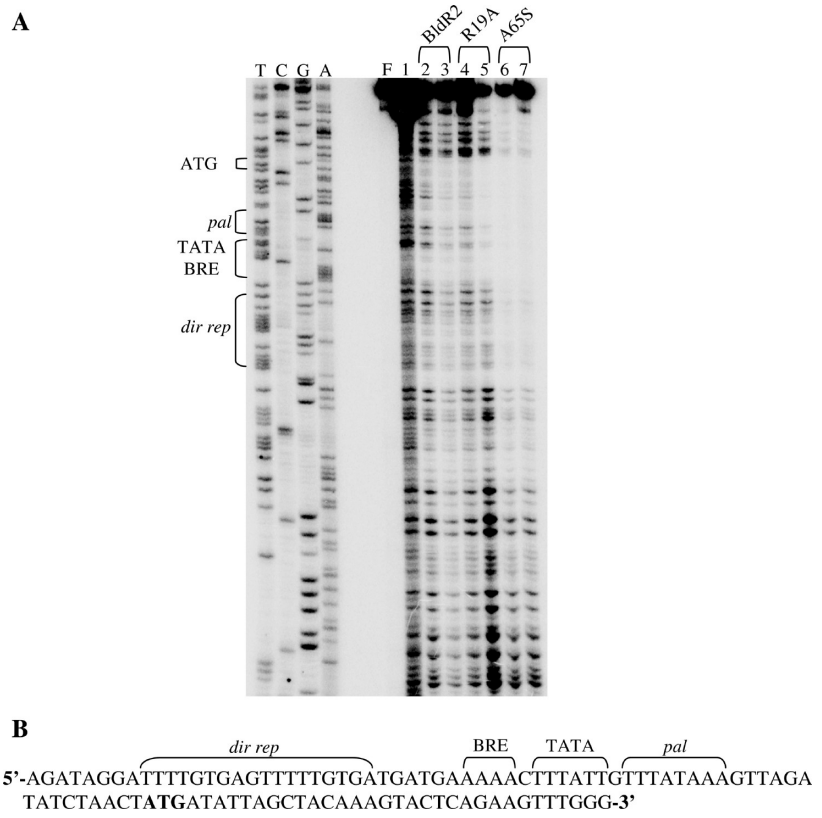

Figure 5. (A) Wild-type and mutant binding sites of the *Sso1082* promoter. DNase I footprinting analysis was performed at the nontemplate strand using 0.0 μg (lane 1), 5 μg (~15 μM, lanes 2, 4, and 6), and 10 μg (lanes 3, 5, and 7) of purified BldR2, R19A, and A65S. DNA fragments were analyzed in parallel with a sequencing reaction (relative lanes are indicated by the corresponding nucleotide positions on the top) by denaturing gel electrophoresis. (B) Positions of the footprints indicated on the nucleotide sequences relative to the transcription and translation start site.

With the aim of precisely positioning the binding sites of BldR2 at its own promoter, a DNase I footprinting analysis was undertaken. As shown in Figure 5A, BldR2, R19A, and A65S protect a region of ~40 bp extending from the pseudopalindromic TATA-BRE sequences to the ATG start codon and containing a 8 bp TTTATAAA palindromic site (Figure 5B). The extent of protection suggests that more than one BldR2 dimer could associate to target DNA. Furthermore, these results prove the presence of regulatory sites in the BldR2 promoter that could function for its in vivo autoregulation. Interestingly, the A65S mutant gave an even more extended footprint; in fact, it protected a further region of 17 bp located more upstream of the TATA box, containing the direct repeat TTTTGTGAgtTTTTGTGA (Figure 5B). This evidence could imply that the introduction of a serine enhances the DNA binding affinity by modifying the recognition sequence.

To analyze the DNA binding behavior of BldR2 upon addition of putative phenolic ligands, we performed EMSAs in which formation of the complex of BldR2 and the mutants with the *Sso1082S* promoter was tested after preincubation of the proteins with increasing concentrations of salicylate and benzaldehyde. The first ligand was chosen because it was demonstrated to be the negative effector of several MarR homologues,[17,22,41] while the second was known to interact positively with the BldR factor in *S. solfataricus*.[25]

The results are shown in Figure 6A: an inhibition of complex formation starts at ~10 mM salicylate (lane 5), while the benzaldehyde was slightly less effective (Figure 6B). In fact, release of BldR2 from its own promoter could be observed from ~30 mM benzaldehyde (lane 6).

DNA binding by the mutant A65S was also affected in the presence of the tested ligands (Figure 6C,D) to a similar extent; in addition, we observed a further band above that of the free DNA, which was interpreted as a partial dissociation of the DNA−protein complex upon ligand interaction.

Taken together, these data indicate that salicylate and benzaldehyde are low-affinity ligands of BldR2 that associate with the protein to attenuate DNA binding.

Conformational Stability of Dimeric BldR2. According to its hyperthermophilic origin, BldR2 has proved to be highly thermostable and resistant to the GuHCl denaturing action as supported by detailed investigation of its conformational stability by means of CD and fluorescence measurements. Figure 7 shows the CD spectra of BldR2 in the far-UV region at 25 °C (spectrum a) and 105 °C (spectrum b). From the latter spectrum, it appears that BldR2 is still folded at that high temperature; in fact, it retains the characteristic minima at 222 and 208 nm with a small decrease in the CD band intensities. The complete disappearance of the canonical CD bands occurs when the protein is incubated for 24 h with 7 M GuHCl (spectrum c). The analysis of the CD spectrum at 25 °C, performed using Dichroweb,[37] suggested that BldR2 contains 66% α-helix and 9% β-sheet; these values closely resemble those obtained from the X-ray structure of the homologous protein, BldR.[24,25] The near-UV CD spectrum of BldR2 is reported in the inset of Figure 7. It also suggested that the protein possesses a well-defined conformation at 25 °C in buffer

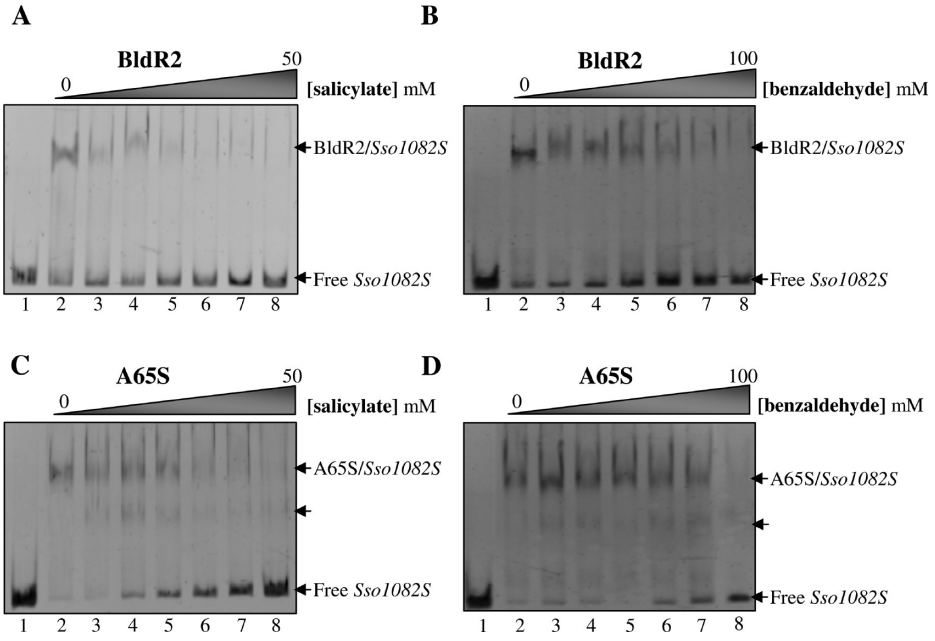

Figure 6. Formation of BldR2−*Sso1082S* and A65S−*Sso1082S* complexes in the presence of salicylate and benzaldehyde. (A and B) *Sso1082S* (150 nM) and BldR2 (16 μM) titrated with increasing concentrations of salicylate (A) and benzaldehyde (B): lane 1, DNA fragment; lane 2, *Sso1082S* incubated with BldR2; lanes 3−8, *Sso1082S* and BldR2 incubated with 3, 5, 10, 20, 30, and 50 mM salicylate (A) and 3, 10, 20, 30, 50, and 100 mM benzaldehyde (B), respectively. (C and D) *Sso1082S* (150 nM) and A65S (0.2 μM) titrated with increasing concentrations of salicylate (C) and benzaldehyde (D): lane 1, DNA fragment; lane 2, *Sso1082S* incubated with A65S; lanes 3−8, *Sso1082S* and A65S incubated with 3, 5, 10, 20, 30, and 50 mM salicylate (C) and 3, 10, 20, 30, 50, and 100 mM benzaldehyde (D), respectively.

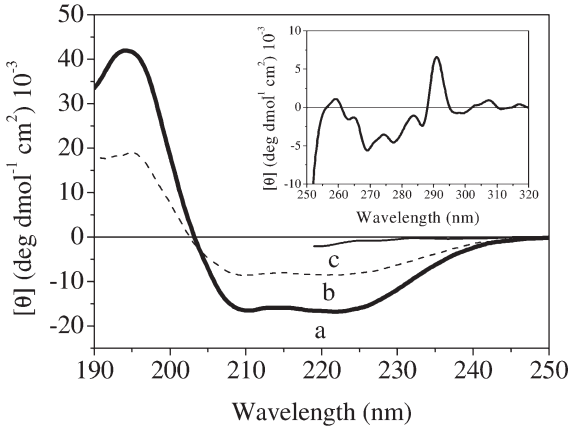

Figure 7. (A) Far-UV CD spectra of BldR2. Spectra were recorded at 25 °C (a, —), 105 °C (b, ---), and 25 °C after incubation for 24 h with 7 M GuHCl (c, —). The inset shows the near-UV CD spectrum of BldR2 (—). The protein concentrations used to acquire the spectra are 2.4 and 20 μM in the far- and near-UV regions, respectively.

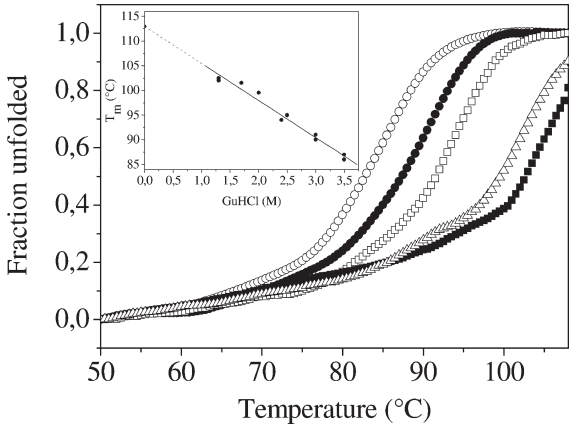

Figure 8. Thermal denaturation curves of BldR2 at a fixed concentration of 2.4 μM, in 20 mM sodium phosphate (pH 7.5) in the presence of 0 (■), 1.3 (△), 2.4 (□), 3 (●) and 3.5 M GuHCl (○). The curves were obtained by recording the changes in the molar ellipticity at 222 nm as a function of temperature. The inset shows the dependence of the melting temperature T_m on GuHCl concentration; via linear extrapolation, a value for T_m in the absence of the denaturant agent was estimated.

solution. The CD spectra of both mutants A65S and R19A were found to be very similar to those of BldR2, suggesting that the secondary and tertiary structure are not affected by the mutations (Figure S3 of the Supporting Information).

Thermal Unfolding. Changes in the far-UV CD signal at 222 nm have been used to follow the thermal unfolding of BldR2 in 20 mM sodium phosphate buffer (pH 7.5). Because of the very high thermal stability, it was not possible to obtain a complete thermal unfolding curve as the transition is not yet finished at 105 °C [see the filled squares (■) in Figure 8], and the instrumental setup cannot work at temperatures higher than 110 °C. To obtain complete thermal denaturation curves, solutions of BldR2 at a fixed final concentration of 2.4 μM were incubated with increasing GuHCl concentrations to progressively destabilize the native state. The corresponding thermal denaturation curves are collected in Figure 8, and the denaturation temperatures obtained were as follows: 102 °C at 1.3 M GuHCl, 96 °C at 2.4 M GuHCl, 91 °C at 3 M GuHCl, and 85 °C at 3.5 M GuHCl. Via linear extrapolation of these numbers up to 0 M GuHCl, the estimated denaturation temperature of BldR2

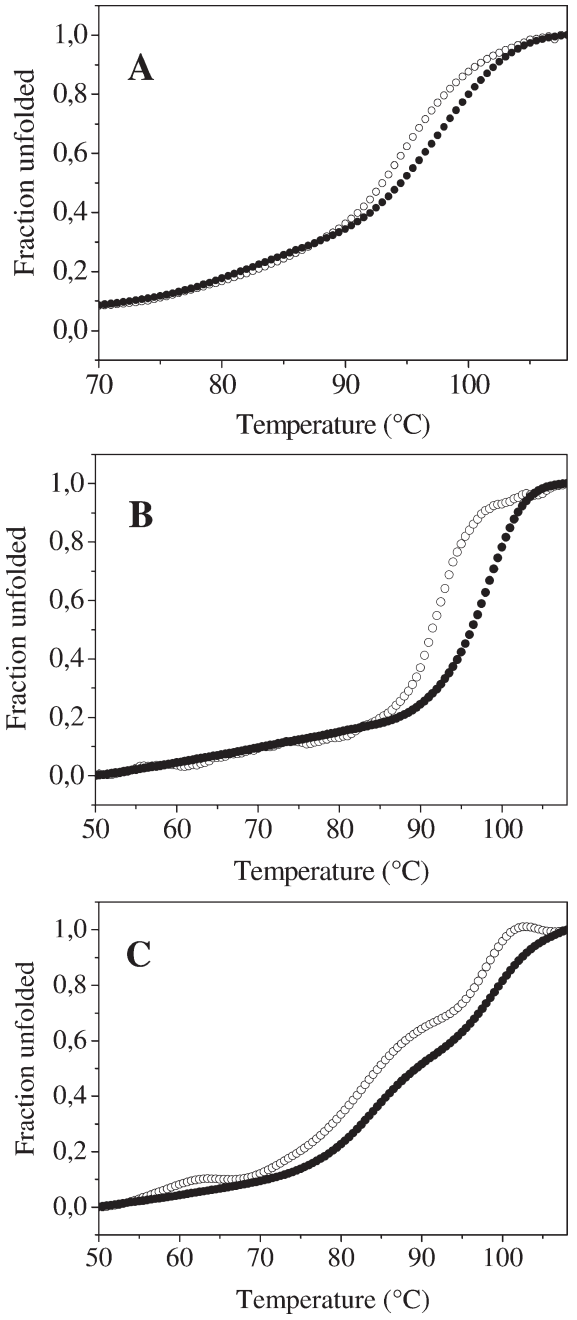

Figure 9. (A) Concentration dependence of BldR2 thermal denaturation, in the presence of 2.4 M GuHCl. Protein concentrations were 1.5 (○) and 9 μM (●), and the T_m shifted from 94.5 to 97.5 °C. (B) Concentration dependence of A65S thermal denaturation, in the presence of 2.4 M GuHCl. Protein concentrations were 0.9 (○) and 9 μM (●), and the T_m shifted from 92.5 to 98 °C. (C) Concentration dependence of R19A thermal denaturation, in the presence of 2.4 M GuHCl. Protein concentrations were 0.9 (○) and 9 μM (●).

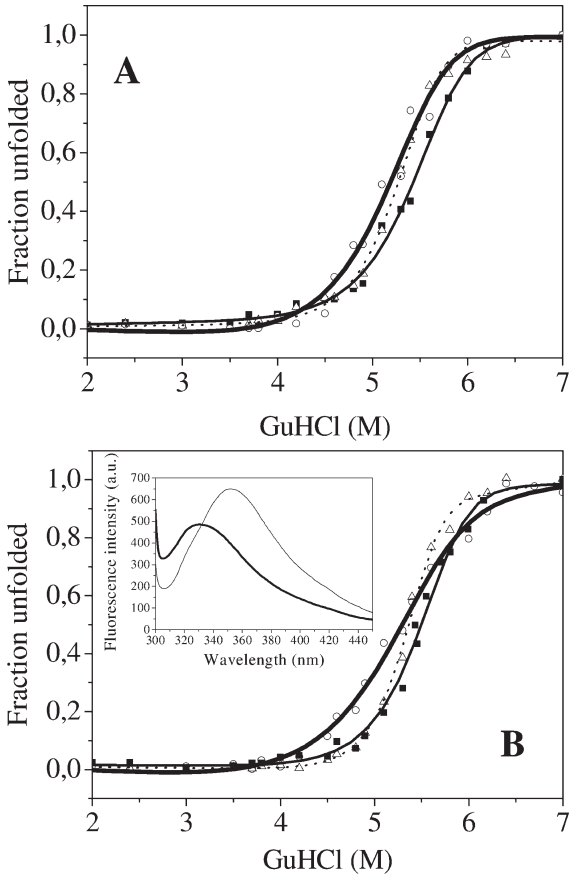

Figure 10. (A) GuHCl-induced unfolding curves of BldR2 (■), A65S (△), and R19A (○), obtained by recording the molar ellipticity at 230 nm and 25 °C. (B) Change in the fluorescence intensity at 336 nm and 25 °C. The lines are the best fits of the curves performed as described in Materials and Methods (inset of Figure 5B). Fluorescence emission spectra of native BldR2 in buffer solution (pH 7.5) (○) and in the presence of 7 M GuHCl (●) at 25 °C.

is 113 ± 1 °C (inset of Figure 8). Figure 9 shows the dependence of the denaturation temperature of BldR2 and its mutants, A65S and R19A, in the presence of 2.4 M GuHCl at two different protein concentrations. For BldR2 and A65S, we observed a shift in the denaturation temperature in a single sigmoid-shaped curve indicative of a two-state dimeric unfolding process (Figure 9A,B), whereas thermal denaturation curves of R19A confirm the concentration dependence but show a biphasic sigmoidal shape with two inflection points (Figure 9C). The thermal denaturation temperature of A65S proved to be very similar to that of BldR2 (111 ± 1 °C). Instead, the biphasic curve of R19A prevented us from correctly estimating the denaturation temperature and strongly suggested a more complex thermal unfolding process (Figure S4 of the Supporting Information). Because thermal denaturation of BldR2 and the mutants is not fully reversible under any of the investigated experimental conditions, no further thermodynamic analysis was performed.

Denaturant-Induced Unfolding. The conformational stability of BldR2 and its mutants against the denaturing action of GuHCl has been investigated at 25 °C in 20 mM sodium phosphate buffer (pH 7.5) by performing CD and fluorescence measurements. It is worth noting that urea cannot be used because BldR2 is extremely resistant to this denaturing agent. The transition curves obtained by recording the molar ellipticity at 230 nm (i.e., detecting the secondary structure stability) and that obtained by recording the fluorescence intensity (tertiary structure) are reported in panels A and B of Figure 10. The inset of Figure 10B shows the comparison of fluorescence emission spectra of BldR2 in the absence and presence of 7 M GuHCl when the protein is completely unfolded according to the

Table 2. Thermodynamic Parameters Obtained by the Analysis of the GuHCl-Induced Unfolding Curves of BldR2 Monitored by the Change in Molar Ellipticity at 230 nm ($[\theta]_{230}$) and of Fluorescence Intensity I_{336} at pH 7.5, 20 mM Sodium Phosphate Buffer, and 25 °C[a]

sample	probe	$\Delta G_U(H_2O)$ (kJ/mol)	m (kJ mol^{-1} M^{-1})	C_m (M)
BldR2	$[\theta]_{230}$	101 ± 5	13 ± 1	5.6
	I_{336}	106 ± 5	14 ± 1	5.6
A65S	$[\theta]_{230}$	116 ± 3	16 ± 1	5.4
	I_{336}	119 ± 4	16 ± 1	5.4
R19A	$[\theta]_{230}$	87 ± 6	11 ± 1	5.2
	I_{336}	82 ± 3	10 ± 1	5.2

[a] Each figure is the average of the values calculated by the nonlinear regression procedure over three independent measurements. Errors are the standard deviations of the fits.

exposure of Trp and Tyr residues to the aqueous solvent. The different spectroscopic probes show superposable transition curves, indicating that both the secondary and tertiary structures are concurrently lost. The GuHCl-induced denaturation curves have a simple sigmoid shape for BldR2, A65S, and R19A, suggesting a cooperative two-state transition between folded dimers and unfolded monomers. The GuHCl-induced unfolding has proven to be reversible: fully unfolded samples showed recovery of spectroscopic features of the native protein after suitable dilution. The GuHCl concentrations at half-completion of the transition are 5.6, 5.4, and 5.2 M for BldR2, A65S, and R19A, respectively, highlighting the very high resistance to the denaturant. As the GuHCl-induced unfolding of BldR2 and A65S and R19A mutants is a reversible process, a thermodynamic analysis of the transitions can be performed. Linear extrapolation of ΔG_U (eq 3) yields the unfolding Gibbs energy in the absence of denaturant [$\Delta G_U(H_2O)$] and the m value; all of the thermodynamic data of the unfolding transitions are listed in Table 2.

DISCUSSION

Because of their function in multidrug resistance and tolerance to highly toxic compounds, MarR transcriptional regulators have been intensely characterized in bacteria and archaea with the aim of understanding the molecular mechanisms of regulated response to such a stress. As many archaea live in hostile environments and are able to defend themselves from a wide variety of stress conditions, they represent an interesting model for determining their ability to survive under rapidly changing conditions. For such organisms, MarR-type regulators might be critical for their adaptation to particular habitats or lifestyles. Intriguingly, the exploration of homologous protein sequences from *Sulfolobales*, including different strains of *S. solfataricus*, *Sulfolobus islandicus*, *S. tokodaii*, and *Sulfolobus acidocaldarius*, revealed that, differently from the majority of bacteria, they all have at least two conserved MarR representatives, indicating the presence of several still uncharacterized regulatory systems involved in multiple-antibiotic resistance. MarR proteins also represent outstanding models for the study of protein stability for several reasons. (i) Many structures from distantly related organisms are available. (ii) They have a dimeric quaternary structure. (iii) They are able to bind DNA only as homodimers.

In this study, an archaeal MarR member, BldR2, was overexpressed in *E. coli* and purified to homogeneity. The protein forms a homodimer in solution and binds specifically to its own promoter region with micromolar affinity, a value that is comparable to those other archaeal MarR members[17,24,25] but is lower than those of many bacterial counterparts.

A primer extension analysis identified a transcription initiation site mapping 45 bp downstream of the first computationally predicted *Sso1082* codon[30] and according to transcriptome mapping.[31] On the basis of our result, a promoter region was found containing consensus BRE-TATA sequences centered at positions −31 and −27 with respect to the transcription start site.

The binding site for BldR2 as determined by DNase I footprinting analysis was found in a region extending from BRE/TATA sequence to the transcription start site. Interestingly, the bound region contains an 8 bp pseudopalindromic sequence (BRE/TATA, AAACTTTA) separated by 3 bp from an 8 bp perfect palindrome (TTTATAAA), suggesting that one BldR2 dimer could bind to each site. Hence, according to the location of the identified basal promoter elements and the BldR2 binding region, it can be proposed that the protein interferes with *Sso1082* transcription by competing with basal transcription factors.

Benzaldehyde and salicylate, known to act as effectors of different MarR proteins at millimolar concentrations, were able to weaken the interaction of BldR2 with its own promoter, suggesting that salicylate and to a lesser extent benzaldehyde could be ligands for BldR2. The low affinity of the effectors for the protein raises questions about their physiological relevance and indicates that other aromatic compounds could be the natural effectors. The in vitro binding results correlated with the in vivo induction of *BldR2* gene expression upon addition of aromatic drugs; the level of gene expression was also increased during the late-log growth phase. The derepression of *Bldr2* both in the presence of aromatic compounds and in late-log growth phase supports a picture in which *BldR2* expression could be regulated by endogenous effectors derived from aromatic catabolic pathways. Hence, BldR2 in vivo would control regulatory mechanisms diverse from those regulated by BldR, which mainly works in the exponential growth phase, and in a different way.[25]

Two single-point mutants, R19A and A65S, were also produced and characterized. The dimeric state of the mutants was confirmed by gel filtration experiments and thermal unfolding at different protein concentrations. The results of the thermodynamic characterization showed that BldR2 possesses a very stable dimeric conformation and that the mutants have also a very high resistance to both temperature and GuHCl denaturing action. In fact, the estimated denaturation temperature of BldR2 is in good agreement with that of the homologous ST1710 from *S. tokodaii*, obtained by differential scanning calorimetry[17] and of the dimeric protein ORF56 from *S. islandicus*.[40] The monophasic temperature-induced unfolding curve of the wild-type protein suggested that the denaturation mechanism occurs in the absence of detectable equilibrium intermediates. This behavior is conserved in mutant A65S, suggesting that the mutation does not affect the protein global stability in solution. Interestingly, mutant R19A shows a biphasic sigmoid-shaped thermally induced unfolding curve. This finding suggests that, in this case, a more complex process occurs, going through the formation of stable intermediate species. On the basis of those results, it is tempting to speculate that residue R19 could be involved in important stabilizing interactions in the dimerization region of the protein, in a way that is reminiscent of what happens in the BldR protein. In fact, in BldR the conserved Arg19 residue of one monomer sets up a strong H bond (distance of 3 Å) with Tyr60 of the other

monomer.[24] The temperature-induced unfolding process is not reversible for all of the studied protein samples; this thermal irreversibility seems to be a common feature of MarR family members. In fact it was also found for the mesophilic HucR from *Deinococcus radiodurans*.[41]

The GuHCl-induced unfolding transitions of BldR2, monitored by CD in the far-UV region and fluorescence, are equivalent, indicating that both the protein secondary and tertiary structure are lost at the same time. This allows us to argue that the transition can be described by a two-state model for a dimer. The experimental values of C_m for BldR2 (5.6 M) and mutants A65S (5.4 M) and R19A (5.2 M) indicate that the wild type is more resistant to the denaturant action than the mutants. The Gibbs energy of unfolding (101 kJ mol^{-1}) is in agreement with that of ORF56 from *S. islandicus* (85.1 kJ mol^{-1}).[40,42] A closer analysis of ΔG_U and m values yields intriguing information about the structural properties of the wild-type protein and its mutants. In particular, even if A65S has a C_m value lower than that of BldR2, its m value is higher and, as a consequence, ΔG_U values are very close. Because a higher m value is usually related to a larger change in the accessible surface area (ASA) upon unfolding, we can argue that the unfolded conformation of the A65S mutant may be more exposed to the solvent.

Another interesting finding is represented by the denaturant-induced unfolding results of R19A that clearly show a simple sigmoid-shaped curve quite different from the biphasic profile obtained for the temperature unfolding curves. The result of the interpolation procedure, based on a simple two-state model, gives an overall lower stability of R19A compared to that of the wild-type protein; it is possible that this value represents an underestimation mainly caused by the choice of the model. In fact, it has been reported previously[43] that the presence of intermediate species in the chemically induced unfolding could not produce any dramatic perturbation in the monophasic unfolding curve, but in that case, the assumption of a two-state model would underestimate the Gibbs energy and the m value.[43] This conclusion fully agrees with the scenario that we previously anticipated on the basis of the thermal experiments in which Arg19 represents an important player in the stabilization of the dimer. Taken together, these results raise the possibility that a simple two-state model could not fully describe the BldR2 denaturation process. Possibly, the equilibrium unfolding of the BldR2 dimer could be described as an apparent two-state reversible reaction, in which unfolding and dissociation are coupled processes. This apparent two-state reaction seems to be confirmed by A65S behavior, while for R19A, the unfolding and dissociation processes seem to be separated, because of the key position of the arginine residue in the dimerization domain.

The structure of the archaeal ST1710−DNA complex and a molecular model of the BldR−DNA complex showed that serine 65 was, in both cases, a critical residue for protein−DNA interaction acting as both a donor and an acceptor of H-bonds with its target DNA. Interestingly, the Ser68 in the bacterial OhrR of *Bacillus subtilis* was also found to make contacts with the major groove of the DNA molecule.[44] In our study, the characterization of the DNA binding properties of the A65S mutant highlighted Ser65 as a key amino acid; in fact, this single-amino acid substitution was able not only to increase the extent of protein−DNA interaction by ∼70-fold but also to cause its binding to a further sequence that is a direct repeat located immediately upstream the TATA/BRE sequence in the *Sso1082* promoter. In archaea, binding by transcriptional regulators to sequences in that position has been proven to be associated with a transcriptional activation.[25,45]

This evidence suggests that the serine residue would allow the formation of an additional interaction with DNA responsible for an extension of the recognition sequence; this would cause a modification both in the binding mechanism and in the sequence specificity. On the basis of this observation, we can also hypothesize that this difference could correlate with the different proposed in vivo physiological roles of the two BldR proteins and depict A65S as a protein intermediate between a repressor (BldR2) and an activator (BldR).

In conclusion, we propose for BldR2 a role in its autoregulation, but further analyses are required to understand the overall mechanism of regulation by BldR2, which would include a deeper investigation of the in vivo function of multiple transcription start sites, a genome-wide identification of target genes and natural ligands, and the analysis of *BldR*$^-$ and *BldR2*$^-$ mutant cells. Furthermore, this study highlights the idea that the identification of key residues involved in dimer stability may contribute to our understanding of the structural−functional relationship in the MarR family, because it is known that mutations in the dimerization domain are critical for the transcriptional regulation of MarR members.[19] Moreover, given that mutations in the DNA binding domain can increase antibiotic tolerance,[46] we also suggest that knowledge of amino acids involved in DNA recognition may provide a remarkable starting point for the design of engineered MarR regulators acting as innovative therapeutic tools.

■ ASSOCIATED CONTENT

Supporting Information. A densitometric analysis of a Northern blot, gel filtration profiles, far-UV CD spectra, and thermal denaturation curves at different GuHCl concentrations of A65S and R19A. This material is available free of charge via the Internet at http://pubs.acs.org.

■ AUTHOR INFORMATION

Corresponding Author

*Phone: +39081679167 (G.F.) or +39081674255 (P.D.V.). Fax: +39081679053. E-mail: fiogabri@unina.it (G.F.) or pompea.delvecchio@unina.it (P.D.V.).

Funding Sources

This work was supported by MIUR-PRIN (Ministero dell'Istruzione, dell'Università e della Ricerca Scientifica-Progetti di Ricerca di Interesse Nazionale) (Grant 2008, CUP: E61J100000200001). The Centro Interdipartimentale di Metodologie Chimico Fisiche (CIMCF, University of Naples Federico II) is gratefully acknowledged for providing the spectrometers. L.M. is a fellow of the European Molecular Biology Organization (EMBO).

■ ACKNOWLEDGMENT

We acknowledge Dr. Raffaele Ronca for helpful discussion, Dr. Patrizia Contursi for critically reading the manuscript, and Dr. Omri Wurtzel for precious explanations about *S. solfataricus* transcriptomic data.

■ ABBREVIATIONS

BldR2, MarR member from *S. solfataricus*; IPTG, isopropyl 1-thio-β-D-galactopyranoside; SDS−PAGE, sodium dodecyl sulfate−polyacrylamide gel electrophoresis; EMSA, electrophoretic mobility shift assay; GuHCl, guanidine hydrochloride; CD, circular dichroism.

■ REFERENCES

(1) Wheelis, M. L., Kandler, O., and Woese, C. R. (1992) On the nature of global classification. *Proc. Natl. Acad. Sci. U.S.A. 89*, 2930–2934.

(2) Grabowski, B., and Kelman, Z. (2003) Archeal DNA replication: Eukaryal proteins in a bacterial context. *Annu. Rev. Microbiol. 57*, 487–516.

(3) Verhees, C. H., Kengen, S. W., Tuininga, J. E., Schut, G. J., Adams, M. W., De Vos, W. M., and Van Der Oost, J. (2003) The unique features of glycolytic pathways in Archaea. *Biochem. J. 375*, 231–246.

(4) van de Vossenberg, J. L., Driessen, A. J., and Konings, W. N. (1998) The essence of being extremophilic: The role of the unique archaeal membrane lipids. *Extremophiles 2*, 163–170.

(5) Geiduschek, E. P., and Ouhammouch, M. (2005) Archaeal transcription and its regulators. *Mol. Microbiol. 56*, 1397–1407.

(6) Hirata, A., Klein, B. J., and Murakami, K. S. (2008) The X-ray crystal structure of RNA polymerase from Archaea. *Nature 451*, 851–854.

(7) Ramos, A., Raven, N., Sharp, R. J., Bartolucci, S., Rossi, M., Cannio, R., Lebbink, J., Van Der Oost, J., De Vos, W. M., and Santos, H. (1997) Stabilization of Enzymes against Thermal Stress and Freeze-Drying by Mannosylglycerate. *Appl. Environ. Microbiol. 63*, 4020–4025.

(8) Jaenicke, R., and Zavodszky, P. (1990) Proteins under extreme physical conditions. *FEBS Lett. 268*, 344–349.

(9) Razvi, A., and Scholtz, J. M. (2006) Lessons in stability from thermophilic proteins. *Protein Sci. 15*, 1569–1578.

(10) Pedone, E., Bartolucci, S., and Fiorentino, G. (2004) Sensing and adapting to environmental stress: The archaeal tactic. *Front. Biosci. 9*, 2909–2926.

(11) Schelert, J., Drozda, M., Dixit, V., Dillman, A., and Blum, P. (2006) Regulation of mercury resistance in the crenarchaeote *Sulfolobus solfataricus*. *J. Bacteriol. 188*, 7141–7150.

(12) Limauro, D., Pedone, E., Pirone, L., and Bartolucci, S. (2006) Identification and characterization of 1-Cys peroxiredoxin from *Sulfolobus solfataricus* and its involvement in the response to oxidative stress. *FEBS J. 273*, 721–731.

(13) Wilkinson, S. P., and Grove, A. (2006) Ligand-responsive transcriptional regulation by members of the MarR family of winged helix proteins. *Curr. Issues Mol. Biol. 8*, 51–62.

(14) Newberry, K. J., Fuangthong, M., Panmanee, W., Mongkolsuk, S., and Brennan, R. G. (2007) Structural mechanism of organic hydroperoxide induction of the transcription regulator OhrR. *Mol. Cell 28*, 652–664.

(15) Alekshun, M. N., Levy, S. B., Mealy, T. R., Seaton, B. A., and Head, J. F. (2001) The crystal structure of MarR, a regulator of multiple antibiotic resistance, at 2.3 Å resolution. *Nat. Struct. Biol. 8*, 710–714.

(16) Perera, I. C., and Grove, A. (2010) Molecular mechanisms of ligand-mediated attenuation of DNA binding by MarR family transcriptional regulators. *J. Mol. Cell Biol. 2*, 243–254.

(17) Kumarevel, T., Tanaka, T., Umehara, T., and Yokoyama, S. (2009) ST1710-DNA complex crystal structure reveals the DNA binding mechanism of the MarR family of regulators. *Nucleic Acids Res. 37*, 4723–4735.

(18) Perera, I. C., Lee, Y. H., Wilkinson, S. P., and Grove, A. (2009) Mechanism for attenuation of DNA binding by MarR family transcriptional regulators by small molecule ligands. *J. Mol. Biol. 390*, 1019–1029.

(19) Okada, N., Oi, Y., Takeda-Shitaka, M., Kanou, K., Umeyama, H., Haneda, T., Miki, T., Hosoya, S., and Danbara, H. (2007) Identification of amino acid residues of *Salmonella* SlyA that are critical for transcriptional regulation. *Microbiology (Reading, U.K.) 153*, 548–560.

(20) Miyazono, K., Tsujimura, M., Kawarabayasi, Y., and Tanokura, M. (2007) Crystal structure of an archaeal homologue of multidrug resistance repressor protein, EmrR, from hyperthermophilic archaea *Sulfolobus tokodaii* strain 7. *Proteins 67*, 1138–1146.

(21) Kumarevel, T., Tanaka, T., Nishio, M., Gopinath, S. C., Takio, K., Shinkai, A., Kumar, P. K., and Yokoyama, S. (2008) Crystal structure of the MarR family regulatory protein, ST1710, from *Sulfolobus tokodaii* strain 7. *J. Struct. Biol. 161*, 9–17.

(22) Saridakis, V., Shahinas, D., Xu, X., and Christendat, D. (2008) Structural insight on the mechanism of regulation of the MarR family of proteins: High-resolution crystal structure of a transcriptional repressor from *Methanobacterium thermoautotrophicum*. *J. Mol. Biol. 377*, 655–667.

(23) Okada, U., Sakai, N., Yao, M., Watanabe, N., and Tanaka, I. (2006) Structural analysis of the transcriptional regulator homolog protein from *Pyrococcus horikoshii* OT3. *Proteins 63*, 1084–1086.

(24) Di Fiore, A., Fiorentino, G., Vitale, R. M., Ronca, R., Amodeo, P., Pedone, C., Bartolucci, S., and De Simone, G. (2009) Structural analysis of BldR from *Sulfolobus solfataricus* provides insights into the molecular basis of transcriptional activation in archaea by MarR family proteins. *J. Mol. Biol. 388*, 559–569.

(25) Fiorentino, G., Ronca, R., Cannio, R., Rossi, M., and Bartolucci, S. (2007) MarR-like transcriptional regulator involved in detoxification of aromatic compounds in *Sulfolobus solfataricus*. *J. Bacteriol. 189*, 7351–7360.

(26) Fiorentino, G., Ronca, R., and Bartolucci, S. (2009) A novel *E. coli* biosensor for detecting aromatic aldehydes based on a responsive inducible archaeal promoter fused to the green fluorescent protein. *Appl. Microbiol. Biotechnol. 82*, 67–77.

(27) Brock, T. D., Brock, K. M., Belly, R. T., and Weiss, R. L. (1972) *Sulfolobus*: A new genus of sulfur-oxidizing bacteria living at low pH and high temperature. *Arch. Mikrobiol. 84*, 54–68.

(28) Cannio, R., Fiorentino, G., Rossi, M., and Bartolucci, S. (1999) The alcohol dehydrogenase gene: Distribution among *Sulfolobales* and regulation in *Sulfolobus solfataricus*. *FEMS Microbiol. Lett. 170*, 31–39.

(29) Limauro, D., Falciatore, A., Basso, A. L., Forlani, G., and De Felice, M. (1996) Proline biosynthesis in *Streptococcus thermophilus*: Characterization of the proBA operon and its products. *Microbiology (Reading, U.K.) 142* (Part 11), 3275–3282.

(30) She, Q., Singh, R. K., Confalonieri, F., Zivanovic, Y., Allard, G., Awayez, M. J., Chan-Weiher, C. C., Clausen, I. G., Curtis, B. A., De Moors, A., Erauso, G., Fletcher, C., Gordon, P. M., Heikamp-de Jong, I., Jeffries, A. C., Kozera, C. J., Medina, N., Peng, X., Thi-Ngoc, H. P., Redder, P., Schenk, M. E., Theriault, C., Tolstrup, N., Charlebois, R. L., Doolittle, W. F., Duguet, M., Gaasterland, T., Garrett, R. A., Ragan, M. A., Sensen, C. W., and Van der Oost, J. (2001) The complete genome of the crenarchaeon *Sulfolobus solfataricus* P2. *Proc. Natl. Acad. Sci. U.S.A. 98*, 7835–7840.

(31) Wurtzel, O., Sapra, R., Chen, F., Zhu, Y., Simmons, B. A., and Sorek, R. (2010) A single-base resolution map of an archaeal transcriptome. *Genome Res. 20*, 133–141.

(32) Notredame, C., Higgins, D. G., and Heringa, J. (2000) T-Coffee: A novel method for fast and accurate multiple sequence alignment. *J. Mol. Biol. 302*, 205–217.

(33) Lambert, C., Leonard, N., De Bolle, X., and Depiereux, E. (2002) ESyPred3D: Prediction of proteins 3D structures. *Bioinformatics 18*, 1250–1256.

(34) Bradford, M. M. (1976) A rapid and sensitive method for the quantitation of microgram quantities of protein utilizing the principle of protein-dye binding. *Anal. Biochem. 72*, 248–254.

(35) Gill, S. C., and von Hippel, P. H. (1989) Calculation of protein extinction coefficients from amino acid sequence data. *Anal. Biochem. 182*, 319–326.

(36) Compton, L. A., and Johnson, W. C., Jr. (1986) Analysis of protein circular dichroism spectra for secondary structure using a simple matrix multiplication. *Anal. Biochem. 155*, 155–167.

(37) Whitmore, L., and Wallace, B. A. (2004) DICHROWEB, an online server for protein secondary structure analyses from circular dichroism spectroscopic data. *Nucleic Acids Res. 32*, W668–W673.

(38) Pace, C. N. (1986) Determination and analysis of urea and guanidine hydrochloride denaturation curves. *Methods Enzymol. 131*, 266–280.

(39) Tanford, C. (1970) Protein denaturation. C. Theoretical models for the mechanism of denaturation. *Adv. Protein Chem. 24*, 1–95.

(40) Zeeb, M., Lipps, G., Lilie, H., and Balbach, J. (2004) Folding and association of an extremely stable dimeric protein from *Sulfolobus islandicus*. *J. Mol. Biol. 336*, 227–240.

(41) Wilkinson, S. P., and Grove, A. (2004) HucR, a novel uric acid-responsive member of the MarR family of transcriptional regulators from *Deinococcus radiodurans*. *J. Biol. Chem. 279*, 51442–51450.

(42) Luke, K. A., Higgins, C. L., and Wittung-Stafshede, P. (2007) Thermodynamic stability and folding of proteins from hyperthermophilic organisms. *FEBS J. 274*, 4023–4033.

(43) Soulages, J. L. (1998) Chemical denaturation: Potential impact of undetected intermediates in the free energy of unfolding and m-values obtained from a two-state assumption. *Biophys. J. 75*, 484–492.

(44) Hong, M., Fuangthong, M., Helmann, J. D., and Brennan, R. G. (2005) Structure of an OhrR-ohrA operator complex reveals the DNA binding mechanism of the MarR family. *Mol. Cell 20*, 131–141.

(45) Kessler, A., Sezonov, G., Guijarro, J. I., Desnoues, N., Rose, T., Delepierre, M., Bell, S. D., and Prangishvili, D. (2006) A novel archaeal regulatory protein, Sta1, activates transcription from viral promoters. *Nucleic Acids Res. 34*, 4837–4845.

(46) Kim, J. Y., Inaoka, T., Hirooka, K., Matsuoka, H., Murata, M., Ohki, R., Adachi, Y., Fujita, Y., and Ochi, K. (2009) Identification and characterization of a novel multidrug resistance operon, mdtRP (yusOP), of *Bacillus subtilis*. *J. Bacteriol. 191*, 3273–3281.